

RESEARCH ARTICLE

Attachment performance of stick insects (Phasmatodea) on convex substrates

Thies H. Büscher*, Martin Becker and Stanislav N. Gorb

ABSTRACT

Phasmatodea (stick and leaf insects) are herbivorous insects well camouflaged on plant substrates as a result of cryptic masquerade. Also, their close association with plants has allowed them to adapt to different substrate geometries and surface topographies of the plants they imitate. Stick insects are gaining increasing attention in attachment- and locomotion-focused research. However, most studies experimentally investigating stick insect attachment have been performed either on single attachment pads or on flat surfaces. In contrast, curved surfaces, especially twigs or stems of plants, are dominant substrates for phytophagous insects, but not much is known about the influence of curvature on their attachment. In this study, by combining analysis of tarsal usage with mechanical traction and pull-off force measurements, we investigated the attachment performance on curved substrates with different diameters in two species of stick insects with different tarsal lengths. We provide the first quantitative data for forces generated by stick insects on convex curved substrates and show that the curvature significantly influences attachment ability in both species. Within the studied range of substrate curvatures, traction force decreases and pull-off force increases with increasing curvature. Shorter tarsi demonstrate reduced forces; however, tarsus length only has an influence for diameters thinner than the tarsal length. The attachment force generally depends on the number of tarsi/tarsomeres in contact, tarsus/leg orientation and body posture on the surface. Pull-off force is also influenced by the tibiotarsal angle, with higher pull-off force for lower angles, while traction force is mainly influenced by load, i.e. adduction force.

KEY WORDS: Adhesion, Friction, Biomechanics, Euplantula, Arolium, Tarsal pads

INTRODUCTION

Attachment during locomotion on different kinds of surfaces is a widespread phenomenon in the animal kingdom. Especially in insects, various types of reversible attachment structures, which allow them to hold themselves and to walk on the majority of natural surfaces (Beutel and Gorb, 2001, 2006, 2008), evolved in response to the great variability of natural surfaces (Gorb, 2001; Gorb and Gorb, 2004). Phasmatodea Jacobson and Bianchi 1902, or stick and leaf insects, are a mesodiverse group of large terrestrial insects (Bradler and Buckley, 2018) inhabiting various habitats worldwide (Bedford, 1978; Brock et al., 2019). These herbivorous insects are


strongly adapted to foraging on plants, e.g. exhibiting extreme forms of masquerade crypsis (Robertson et al., 2018), and presumably have co-evolved with plants since pre-angiosperm times (Wang et al., 2014). This process shaped the evolution of the attachment apparatus of phasmids and resulted in diverse adaptations to different surfaces in their habitats (Büscher et al., 2019). As a result, the tarsal attachment apparatus of most stick insects consists of a flexible chain of five tarsomeres, bearing two types of attachment pads and two claws. The tarsal euplantulae, present on the proximal four/five tarsomeres, are used to generate friction and withstand shear forces, and the pretarsal arolium provides adhesion to withstand pull-off forces (Labonte and Federle, 2013). On smooth or micro-rough surfaces, these pads provide attachment due to adhesion and friction forces, whereas on rough surfaces the claws additionally achieve mechanical interlocking (Büscher and Gorb, 2019). Species-specific functional attachment microstructures (AMS) are present on the euplantulae of stick insects and correlate with the different substrates in their natural habitats (Büscher and Gorb, 2017; Büscher et al., 2018a,b, 2019). These structures are reported for at least one species to change during post-embryonic development, in which the animals change their habitat (Gottardo et al., 2015). Previous studies on the attachment performance of stick insects have shown that euplantulae with smooth AMS generate higher forces on smooth surfaces, whereas nubby euplantulae are adapted to micro-rough surfaces (Bußhardt et al., 2012; Büscher and Gorb, 2019).

Most studies on the attachment properties of stick insects have focused on the performance of single attachment pads (Bennemann et al., 2011; Bußhardt et al., 2012; Labonte and Federle, 2013; Labonte et al., 2014) and examined the adhesive and frictional components of attachment in detail. Other studies, focusing on the attachment performance of whole stick insects, investigated the combination of the different pads and claws and their contribution to the overall attachment (Büscher and Gorb, 2019; Labonte et al., 2019). In regard to measurements of actual attachment forces, these studies are limited to investigations of (1) size dependence of attachment in different instars of one species of stick insects (Labonte et al., 2019) and (2) complementary effects of different components of the attachment apparatus in two other species (Büscher and Gorb, 2019). Labonte et al. (2019) have shown that during the ontogeny of stick insects, adhesion scales with contact area in whole-animal measurements, as attachment performance compensates for weight in larger stick insects by the weight-related shear forces produced by sliding of the pads. Büscher and Gorb (2019) investigated the use of all tarsal attachment structures in two species and showed a flexible usage of the attachment pads according to the animal's orientation to the substrate. This study revealed stronger attachment forces on rough substrates by the contribution of claws and on smooth substrates by the contribution of tarsal attachment pads.

Although they provide insight into the functionality of the whole attachment system, all these studies have been carried out on flat

Department of Functional Morphology and Biomechanics, Institute of Zoology, Kiel University, Am Botanischen Garten 9, 24118 Kiel, Germany.

*Author for correspondence (tbuescher@zoologie.uni-kiel.de)

 T.H.B., 0000-0003-0639-4699; S.N.G., 0000-0001-9712-7953

Received 8 April 2020; Accepted 20 July 2020

surfaces. In nature, stick insects face a lot of differently structured surfaces. In particular, curved surfaces, such as branches or twigs of plants, are among the most abundant substrates for stick and leaf insects (Bedford, 1978; Gottardo et al., 2015; Büscher et al., 2019) and have even shaped the appearance of most stick insects (Bedford, 1978; Wang et al., 2014; Bradler and Buckley, 2018). Locomotion on curved substrates implicates different mechanics in comparison to upright walking on flat substrates. Previous studies on other insects have examined some aspects of locomotion on twigs and curved substrates. Studies of different insect species walking on thin stems revealed several strategies of attachment, including the use of pads, claws and additional structures on the tibia enabling attachment to and propulsion along the stems (Gladun and Gorb, 2007; Bußhardt et al., 2014). Measurements of attachment forces showed remarkable differences between the maximal forces on curved surfaces and flat ones for beetles and true bugs (Bußhardt et al., 2014; Voigt et al., 2017, 2019). In these studies, the measured attachment forces were higher on rods in comparison to flat plates of the same material. The attachment performance on curved substrates is different for different radii of curvature in relation to the dimensions of the animal, as it has been shown for frogs that traction is dependent on the diameter of the cylinder the frog tries to ascend (Bijma et al., 2016; Hill et al., 2018).

On smooth flat surfaces, it is known that wide tarsi generate higher attachment forces than slender tarsi in *Stenus* rove beetles (Betz, 2002), demonstrating an influence of tarsus geometry on attachment performance. The performance on different diameters of curved substrates should be dependent on the length of the attachment system instead. The length of the tarsal chain might have an effect on how many attachment pads can be brought into contact with a curved substrate and can further influence the orientation of the attachment pads on the substrate. Friction experiments on the euplantulae of two species of stick insects revealed frictional anisotropy for both smooth and nubby euplantulae (Bußhardt et al., 2012). At a load of 500 μN , the species *Medauroidea extradentata* and *Carausius morosus* both show higher friction in the proximal direction (pull) than in the distal direction (push). The diameter of the structure in relation to the length of the tarsal chain determines how the tarsi can be placed on it (Gladun and Gorb, 2007; Voigt et al., 2017) and, hence, influences the orientation of the animal and the direction of the forces acting on the attachment system.

In this study, we examined the attachment capability of stick insects on surfaces with different levels of curvature. We measured the pull-off and traction forces of the species *Sungaya inexpectata* and *Orestes mouhotii*. These two species differ primarily in body size and in the length of their tarsi (Bücher et al., 2019). Specifically, we aimed to answer the following questions. (1) How does the attachment system of stick insects perform in traction and pull-off on curved substrates with different diameters? (2) Does the length of the tarsus influence attachment ability on surfaces with different degrees of curvature? (3) How do stick insects use the tarsal attachment system during locomotion on curved substrates?

MATERIALS AND METHODS

Animals

The species *Sungaya inexpectata* Zompro 1996 and *Orestes mouhotii* (Bates 1865) were chosen (Fig. 1), as their tarsi differ in the length of the tarsal chain, but not in either their overall tarsal morphology (see Fig. 2) or their euplantular microstructures (Bücher et al., 2019). Females were selected to avoid differences caused by sexual dimorphism. All animals examined in this study

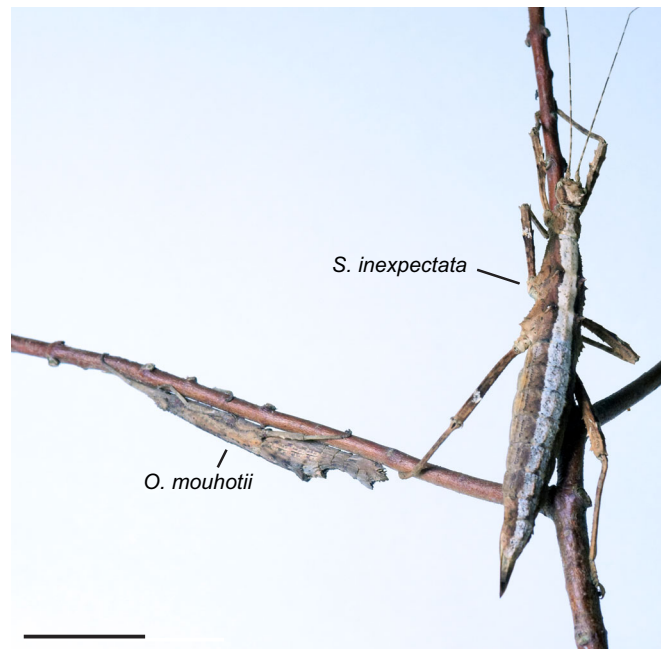


Fig. 1. Species examined in this study. Adult females of *Sungaya inexpectata* and *Orestes mouhotii*. Scale bar: 2 cm.

were obtained from the laboratory cultures of the Department of Functional Morphology and Biomechanics (Kiel University, Germany). They were fed with leaves of bramble (*Rubus* spp.) and hazel (*Corylus avellana*) *ad libitum*. All animals retained a natural day/night cycle. Adult individuals with six intact legs and no visible damage on the attachment pads (using light microscopy) were used. All insects were weighed prior to the measurements to the nearest 100 μg (AG204 Delta Range, Mettler Toledo, Columbus, OH, USA). We used the same specimens for pull-off and traction force measurements and measured their mass on the particular day of the measurement. As the mass of the specimens changed over the course of the experiment, the values reported below correspond to the masses of the individual insects at the time of the measurements.

Scanning electron microscopy

Tarsi of both species were cut off from adult females and fixed in 2.5% glutaraldehyde in PBS buffer for 24 h on ice on a shaker. Afterwards, samples were dried in an ascending ethanol series, critical-point dried and sputter-coated with a 10 nm layer of gold-palladium. The samples were mounted on a rotatable specimen holder (Pohl, 2010) and overview images were obtained using a scanning electron microscope (TM3000, Hitachi High-technologies Corp., Tokyo, Japan) at 15 kV acceleration voltage. The micrographs were processed and measurements of the tarsal segments were conducted using the software Photoshop CS6 (Adobe Systems Inc., San Jose, CA, USA). The tarsi were visualized from the lateral view to measure the length of all tarsomeres (see Fig. 2).

Substrate preparation

As substrates, we used custom-made tubes and plates of acrylic glass. We used four tubes with diameters of 24.8, 11.9, 5 and 2.9 mm to provide substrates that correspond to different abilities of the animals to embrace the tubes. These cylinders correspond to the different geometric characteristics of twigs in the natural habitats,

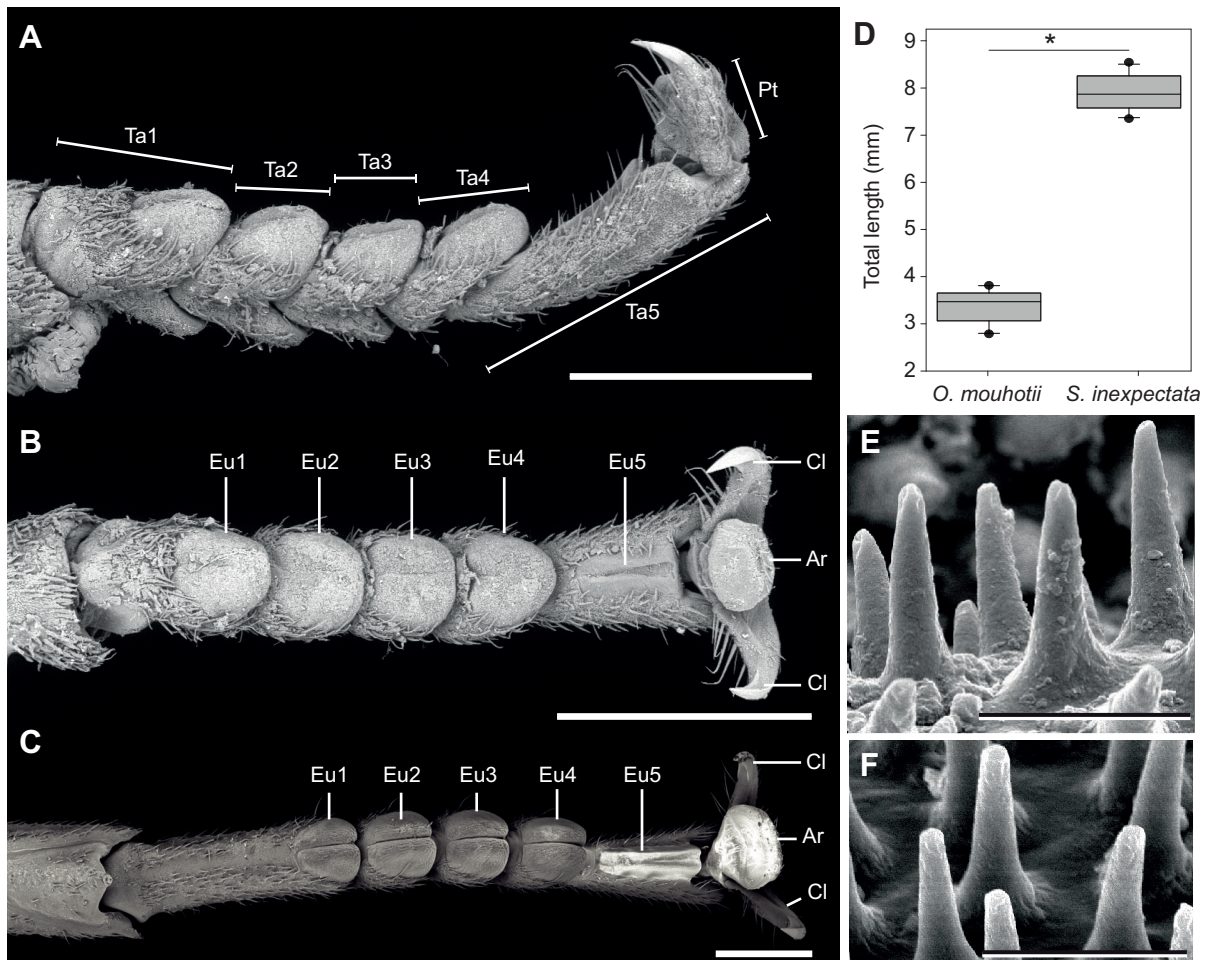


Fig. 2. Tarsal morphology of the examined species. (A–C) Scanning electron micrographs of the right metatarsus of an adult female *O. mouhotii* (A,B) and *Sungaya inexpectata* (C) (A, lateral overview; B,C, ventral overviews). (D) Total tarsal length of the two species (paired *t*-test, $t=-24.26$, d.f.=10, $N_{1,2}=11$, $P<0.001$). Boxes indicate the 25th and 75th percentiles, whiskers are the 10th and 90th percentiles and the line within the boxes shows the median. (E,F) The nubby microstructure on the euplantulae (4th euplantula) of the right metatarsus of an adult female *O. mouhotii* (E) and *S. inexpectata* (F). Ar, arolium; Cl, claw; Eu, euplantula; Pt, pretarsus; Ta, tarsomere. * $P<0.001$. Scale bars: 1 mm (A–C), 4 μm (E,F).

but exclude parameters influencing attachment, like differing roughness, stiffness or surface chemistry. For comparison, we used a flat square plate of acrylic glass. All substrates were cleaned with ethanol prior to the experiment. During the experiments, the substrates were cleaned between measurements to remove potential residuals of attachment pad fluids from the substrates. All substrates had a length of 25 cm, in order to provide sufficient latitude for horizontal pulling.

Force measurements

Attachment forces were measured with a BIOPAC model MP100 and TCI-102 system (BIOPAC Systems, Inc., Goleta, CA, USA), connected to a 100 g force transducer (FORT100, World Precision Instruments, Sarasota, FL, USA). A horse hair was attached to the force transducer and glued with Plasticine to the metanotum of the stick insect. The attachment forces of the insects were measured in the following two directions: vertically (pull-off force) and horizontally (traction force).

Pull-off forces

Specimens of both species (*S. inexpectata* 1.18 ± 0.26 g mean \pm s.d., $N=14$; *O. mouhotii* 0.91 ± 0.22 g, $N=14$) were attached to the force transducer as described above. To pull the insects off the substrate at

an angle of 90 deg, the force transducer was mounted on a micromanipulator (DC 3001R, World Precision Instruments Inc.) with the same setup described by Wohlfart et al. (2014) and employed for stick insects by Büscher and Gorb (2019). One glass tube at a time, or the flat plate, respectively, was fixed below the animal using two clamps. The micromanipulator was manually moved upwards, with a retraction velocity of $2\text{--}4\text{ cm s}^{-1}$, and stretched the horse hair in the vertical direction until the animal detached from the surface (see Fig. 3B).

Traction forces

Specimens of both species (*S. inexpectata* 1.32 ± 0.31 g, $N=14$; *O. mouhotii* 1.05 ± 0.13 g, $N=14$) were attached to the force transducer in the same manner as described above. To measure passive traction force, the force transducer was aligned horizontally at the same height as the insect (see Wolff and Gorb, 2012; Büscher and Gorb, 2019). Each insect was then manually pulled backwards (along its body axis) in the traction direction without detaching it from the surface with a retraction velocity of $2\text{--}5\text{ cm s}^{-1}$ (see Fig. 3A). As both species preferred to walk upright on the flat surface and on the tube with the largest diameter, but walked hanging upside down on the other tubes, the traction forces were measured in accordance with the naturally preferred animal orientation (see below).

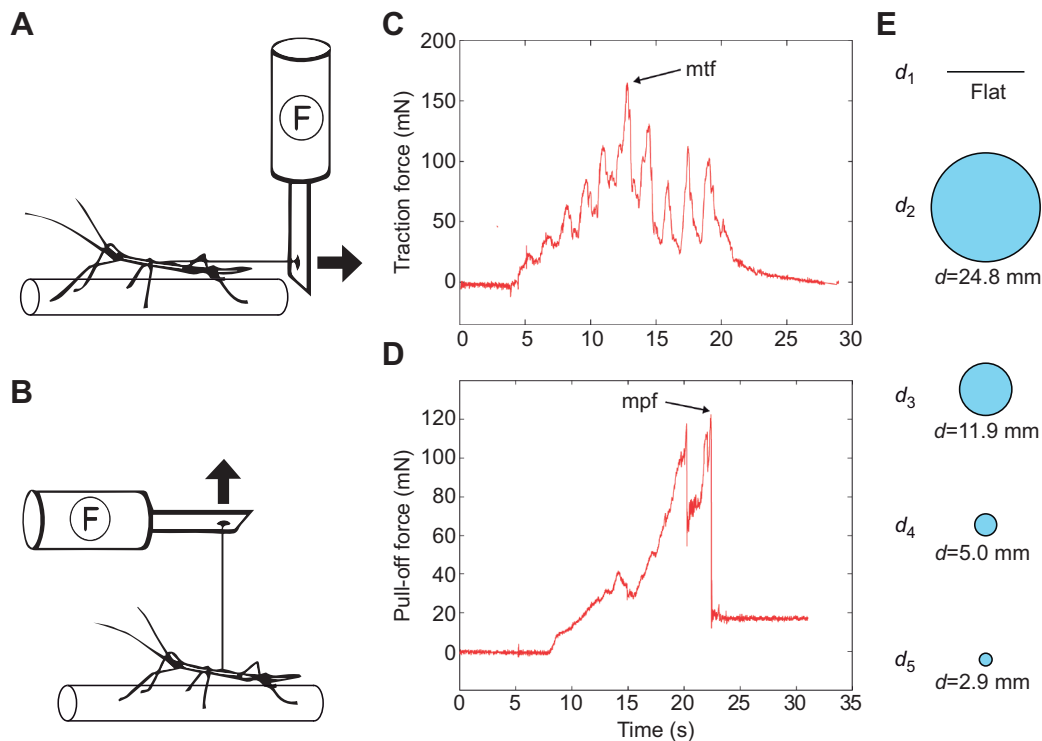


Fig. 3. Experimental setup for traction and pull-off force measurements. (A,B) Schematic setup of force measurements in the traction (A) and pull-off (B) direction. (C,D) Example curves for traction (C) and pull-off force (D). (E) Cross-sections of the flat plate (d_1) and cylindrical substrates used in the experiments: 24.8 mm (d_2), 11.9 mm (d_3), 5 mm (d_4) and 2.9 mm diameter (d_5) tube. mtf, maximum traction force; mpf, maximum pull-off force.

Force data analysis

In both directions, force–time curves were recorded and visualized with the software Acqknowledge 3.7.0 (BIOPAC Systems Inc., Goleta, CA, USA). The maximum peak of the force–time curve was extracted for data analysis (see Fig. 3C,D for example curves). For every direction and every species, the attachment forces for 14 individuals were measured. Every insect was measured 3 times and the median of all three maximum attachment forces was taken. The order of surfaces was randomized for each animal and the order of measured individuals was also randomized during the experiment. All measurements were performed in daylight at 19–21°C and 50–60% relative humidity. Additionally, the behaviour of animals was documented during the measurements.

Videography

To evaluate walking behaviour and leg positioning, adult females of both species were filmed on each surface (*S. inexpectata* 1.24 ± 0.27 g, $N=10$; *O. mouhotii* 1.04 ± 0.13 mg, $N=10$). The animals were filmed with a Nikon D5300 digital camera (Nikon Corp., Tokyo, Japan) equipped with a macro lens (Canon Macro Lens EF 100 mm, Canon Inc., Tokyo, Japan) from the lateral side on all substrates. We analysed (1) the walking gait pattern, (2) the orientation of the specimen in relation to the substrate and (3) the positioning of the tarsi. Therefore, sequences of at least 10 steps were analysed and sequences with disruptions (turns, falls, etc.) were excluded. For the flat substrate, only sequences where the animal walked in a straight line were used. For analysis of the videos, Adobe Premiere Pro CS6 software (Adobe Systems Inc.) was used. To evaluate the walking gait patterns, three general patterns were identified (tripod, quadrupedal/tetrapod, waive gait; see Grabowska et al., 2012; Büscher and Gorb, 2019), based on the number of feet simultaneously in contact with the substrate, with a maximum of

10% of steps deviating from the ground pattern. If more than 10% of steps were observed differing from the ground pattern (e.g. transitions between two gait patterns), we considered these gait pattern sequences as irregular.

Statistical analysis

SigmaPlot 12.0 (Systat Software Inc., San Jose, CA, USA) was used to perform the statistical analyses. Initially, normal distribution (Shapiro–Wilk test) and homoscedasticity (Levene’s test) were tested. The tarsal length and the body weight of both species were compared using a two-tailed *t*-test. The traction and pull-off forces on the five different substrate radii were compared for both species separately using one-way ANOVA and Holm–Šidák’s *post hoc* test, if the data were normally distributed and showed homoscedasticity. Kruskal–Wallis ANOVA on ranks and Tukey’s *post hoc* tests were used if the data were not normally distributed. The safety factors (attachment force per body mass) of the two species on substrates with different radii were compared using *t*-test. For better understanding, the exact test used and the sample size are specified in the relevant sections.

RESULTS

Tarsal morphology

As for the majority of extant Phasmatodea, the tarsi of both species examined consisted of five tarsomeres (see Büscher et al., 2019), each equipped with one euplantula (Fig. 2A–C). The pretarsus bears two claws and an arolium. The tarsi of *S. inexpectata* were significantly longer than the tarsi of *O. mouhotii* (paired *t*-test, $t=-24.26$, d.f.=10, $N_{1,2}=11$, $P<0.001$). The measurements of the length of single tarsomeres and the total length of the tarsus in all specimens are available in Table S1. We did not find significant differences in the total tarsal length between different leg pairs in the

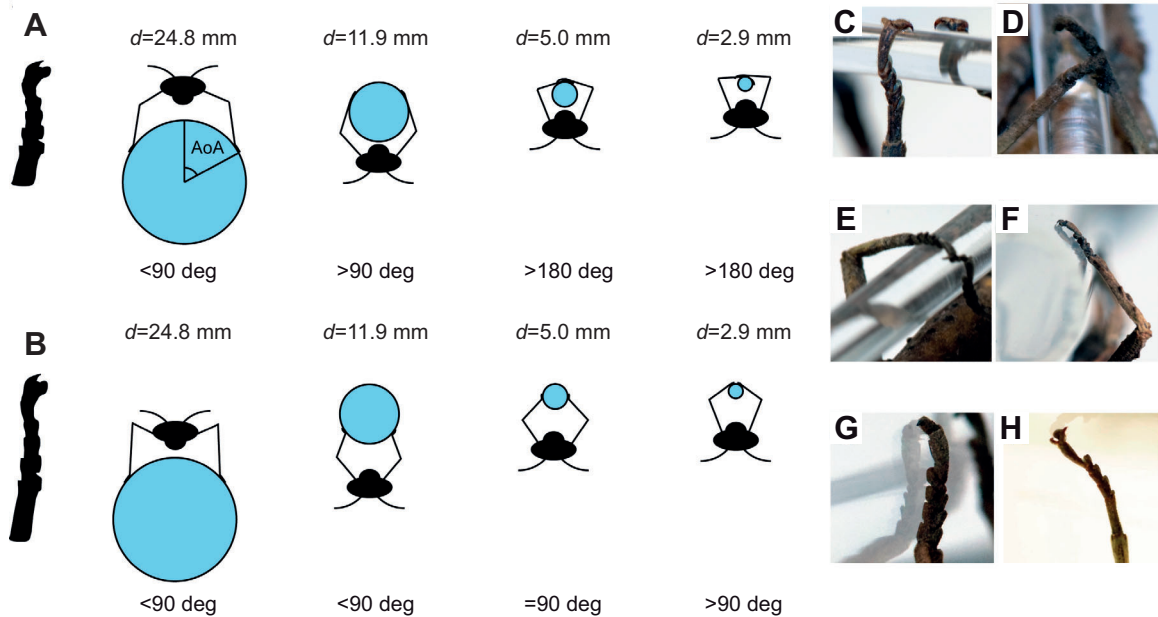


Fig. 4. Posture and leg conformations of both species on the different substrates. (A,B) Body and leg positioning on the different substrate diameters (d) in (A) *O. mouhotii* (short tarsus) and (B) *S. inexpectata* (long tarsus). AoA, angle of attachment, i.e. angle between the centre of the animal (in frontal projection) and the distal-most part of the tarsus (indicated below each animal scheme). (C–H) Images of example tarsal contacts taken in experiments: *S. inexpectata* on $d=2.9$ mm (C); *O. mouhotii* on $d=2.9$ mm (D), $d=5.0$ mm (E), $d=11.9$ mm (F,G); and (H) *S. inexpectata* on $d=11.9$ mm.

two species examined (see Table S2; *S. inexpectata*: Kruskal–Wallis one-way ANOVA; $H=2.455$, $d.f.=2$; $P=0.293$, $N=15$; *O. mouhotii*: Kruskal–Wallis one-way ANOVA; $H=0.0614$, $d.f.=2$, $P=0.97$, $N=15$). The total length of the *S. inexpectata* tarsus (all three leg pairs pooled) was 7.87 ± 0.36 mm (median \pm s.d.) and 3.47 ± 0.34 mm for *O. mouhotii* (see Fig. 2). The major difference in the tarsal morphology between both species was the length of the single tarsomeres. In particular, the basitarsus (Ta1) was longer in *S. inexpectata* (2.91 ± 0.13 mm) than in *O. mouhotii* (1.0 ± 0.1 mm). Both species possess a nubby microstructure on the euplantulae (see Fig. 2), as previously reported (e.g. Büscher et al., 2019). Although the length of the tarsi of the same leg pairs differed between the species, the dimensions of the surface microstructure on the euplantulae were similar (Fig. 2E,F).

Locomotion on curved substrates

The locomotory behaviour on the test substrates differed depending on the degree of their curvature. All tested individuals were analysed to obtain the following data: (1) walking gait pattern, (2) orientation on the substrate, (3) angle of attachment (AoA) and (4) leg configuration (see Fig. 4). The AoA is defined by the centre of the animal in the frontal projection and the distal-most part of the tarsus being in contact with the substrate (Fig. 4A). Both species showed

rather similar behaviour on each test substrate (Table 1). On nearly all substrates, insects employed a tripod walking gait pattern (three legs at once in swing phase). Only on the tube with the smallest diameter did *O. mouhotii* walk more slowly and just moved two legs at once (tetrapod gait) in 80% of the recorded sequences. The same species used tripod gait in 100% of the sequences on all other substrates except the tube with the largest diameter, where it used tetrapod gait in 25% of the sequences. *Sungaya inexpectata* used tripod gait less often, but still in the majority of sequences (Table 1). On the smallest tube (2.9 mm diameter), *S. inexpectata* moved more carefully and used tripod gait in only 40% of the sequences and tetrapod gait in all of the others. On both the 5.0 and 24.8 mm tubes, tripod gait was used in 90% of the sequences and on the flat substrate in 60% of the sequences. All *S. inexpectata* sequences which did not show tripedal walking gait patterns revealed tetrapedal gait patterns.

The same orientation to the substrate was recorded in all individuals of both species. On the 24.8 mm tube, both species walked upright on the tube, attaching at an AoA of <90 deg (Fig. 4B). On the three other tubes, both species walked hanging upside down. This agrees to observations on the species *Aretaon asperrimus* (Frantsevich and Cruse, 1997), which is quite closely related to the species examined herein (Brock et al., 2019). While *S.*

Table 1. Walking pattern and body posture on the test substrates

Substrate diameter (mm)	<i>Sungaya inexpectata</i>			<i>Orestes mouhotii</i>		
	Gait pattern	Body posture		Gait pattern	Body posture	
2.9	Tripod (40%)	Tetrapod (60%)	Hanging down	Tetrapod (80%)	Irregular (20%)	Hanging down
5.0	Tripod (90%)	Tetrapod (10%)	Hanging down	Tripod (100%)		Hanging down
11.9	Tripod (100%)		Hanging down	Tripod (100%)		Hanging down
24.8	Tripod (90%)	Tetrapod (10%)	Standing	Tripod (75%)	Tetrapod (25%)	Standing
Plane	Tripod (60%)	Tetrapod (40%)	Standing	Tripod (100%)		Standing

inexpectata attached at the downside of the 11.9 mm tube at an AoA of <90 deg, *O. mouhotii* revealed AoAs of >90 deg on the same tube. On the smaller tubes, *O. mouhotii* embraced the tubes with higher AoAs than *S. inexpectata* as well. While *O. mouhotii* attached with AoAs of >180 deg on both 5.0 and 2.9 mm diameter tubes, *S. inexpectata* revealed AoAs of 90 deg on 5.0 mm and >90 deg but <180 deg on the 2.9 mm tube. While hanging down, both species attached with AoAs of >90 deg on all substrates with one exception: on the tube with a diameter of 11.9 mm, *S. inexpectata* did not embrace the tube, but attached hanging on the downside. Although the animals kept some distance from the tube while hanging down, their legs were still angled (tibiofemoral joint 90–160 deg). In this posture, only the arolia were employed for attachment (Fig. 4H). In all other situations in which the animals were hanging upside down (11.9 mm for *O. mouhotii*, 5.0 and 2.9 mm for both species), the insects embraced the tubes with AoAs of 90 deg or more. In these postures, animals employed all attachment pads (arolia and euplantulae), except for the fifth euplantula (see Fig. 2A–C), which was used in only a few sequences: on the 5 and 2.9 mm substrates by *S. inexpectata* and only on the 2.9 mm substrate by *O. mouhotii* (Fig. 4C–G). The four proximal euplantulae were used on all curved substrates by both species, except for all individuals of *S. inexpectata*, which used the arolium only on the 11.9 mm substrate (Fig. 4H) and the arolium and the distal-most three euplantulae on the 2.9 mm substrate. Generally, on the flat substrate, both species brought only the

arolium and euplantulae of the third and fourth tarsomeres into contact.

Traction forces

The traction forces, measured via horizontal pulls, revealed lower values for smaller tube diameters for both species. Generally, *S. inexpectata* showed the highest traction force (Fig. 5C) on the 24.8 mm diameter tube (272.38 ± 111.40 mN, median \pm s.d.), lower force on the flat substrate (230.05 ± 97.87 mN) and further decreasing values on decreasing tube diameters (11.9 mm: 220.17 ± 77.92 mN, 5.0 mm: 146.07 ± 53.67 mN, 2.9 mm: 126.97 ± 67.06 mN). Statistical analysis, however, revealed significant differences primarily between the traction forces on larger tube diameters and the flat substrate in comparison with smaller tube diameters (one-way ANOVA, $F=7.3$, $N=14$, $P<0.001$). In detail, the traction forces on the smallest tube (2.9 mm diameter) were significantly lower than those on the flat substrate (Holm–Šidák test, $P=0.015$), the 24.8 mm diameter tube (Holm–Šidák test, $P<0.001$) and the 11.9 mm diameter tube (Holm–Šidák test, $P=0.032$), but not different from those on the 5.0 mm diameter tube (Holm–Šidák test, $P=0.798$). The traction forces generated on the 5.0 mm diameter tube were significantly lower in comparison to those on the largest tube (Holm–Šidák test, $P=0.002$).

A similar trend was observed in *O. mouhotii* (Fig. 5A), with the highest mean traction forces of 210.21 ± 71.96 mN on the 24.8 mm diameter tube, 188.28 ± 90.47 mN on the flat substrate, $177.97 \pm$

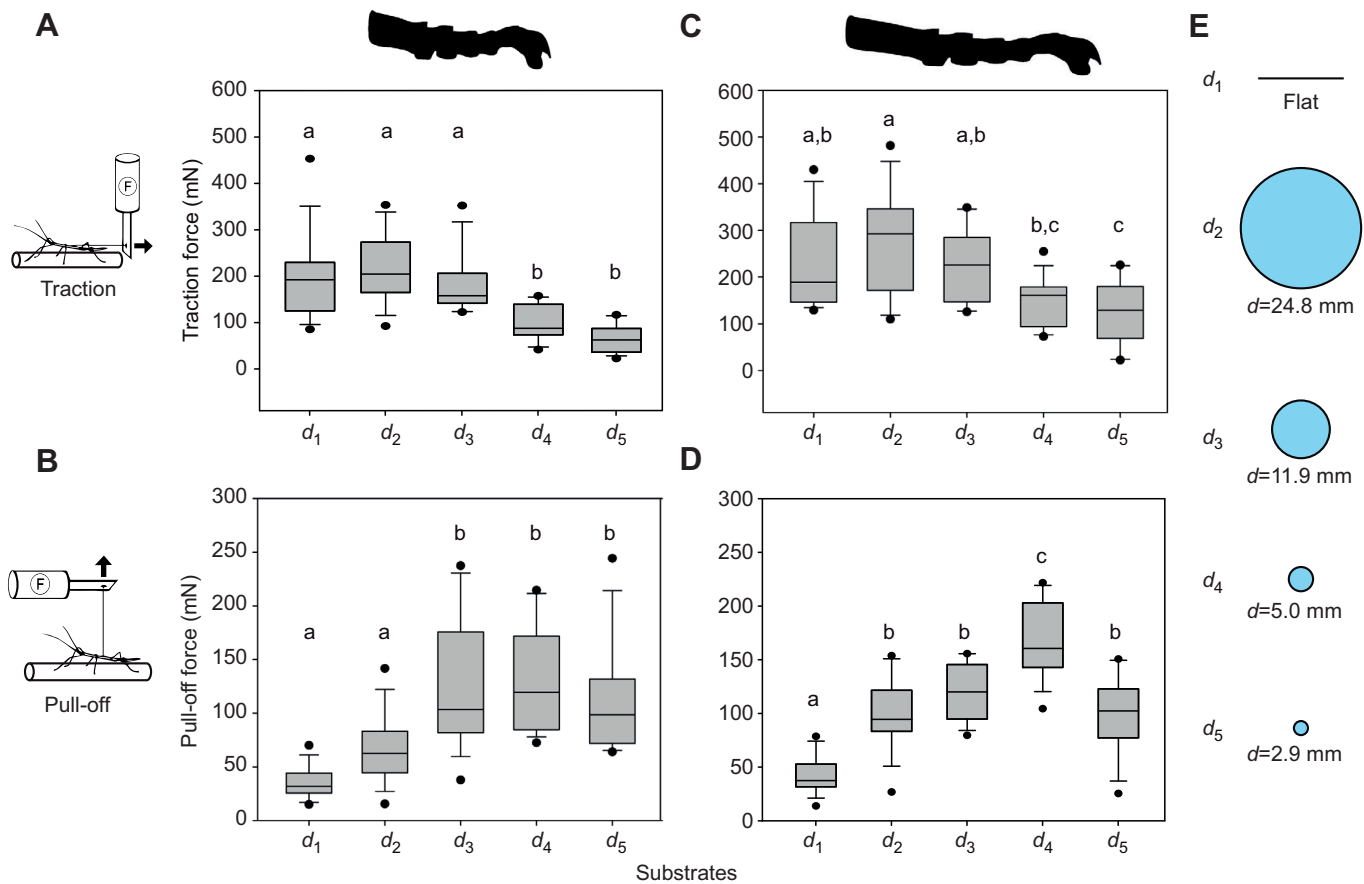


Fig. 5. Traction and pull-off force for the two species on the differently curved substrates. (A,B) *Orestes mouhotii* ($N=14$) traction force (A) and pull-off force (B). (C,D) *Sungaya inexpectata* ($N=14$) traction force (C) and pull-off force (D). Groups with different lowercase letters are statistically different. Boxes indicate the 25th and 75th percentiles, whiskers are the 10th and 90th percentiles and the line within the boxes shows the median. (E) The different substrates.

65.08 mN on the 11.9 mm diameter tube and 93.20 ± 37.48 mN on the 5.0 mm diameter tube. The lowest traction force of 60.12 ± 31.74 mN was measured on the 2.9 mm tube. In general, *O. mouhotii* generated higher traction on the substrates with the largest diameters (i.e. lowest curvature) and lower traction on the smallest diameter tube. Kruskal–Wallis one-way ANOVA ($H=41.82$, d.f.=4, $N=14$, $P=0.001$) revealed a significantly higher traction force on the flat substrate and the two largest tubes (24.8 mm diameter and 11.9 mm diameter) in comparison to the 5.0 mm and 2.9 mm tubes (Tukey's test, $P<0.05$).

Pull-off forces

The pull-off forces generated by *S. inexpectata* (Fig. 5D) were highest on the 5.0 mm tube with 166.41 ± 34.93 mN (mean \pm s.d.) (one-way ANOVA, $F=30.65$, $N=14$, $P<0.001$; Holm–Šidák test, $P<0.001$). The performance on this tube was significantly higher than on the other tubes (2.9 mm: 99.73 ± 37.57 mN, 11.9 mm: 119.61 ± 26.39 mN, 24.8 mm: 98.08 ± 33.02 mN), which were not significantly different from each other (one-way ANOVA, $F=30.65$, $N=14$, $P<0.001$; Holm–Šidák test, $P>0.05$). The pull-off forces on the flat substrate were significantly lower than on all other substrates (40.14 ± 17.42 mN; one-way ANOVA, $F=30.65$, $N=14$, $P<0.001$; Holm–Šidák test, $P<0.001$). For *O. mouhotii*, the pull-off forces (Fig. 5B) were significantly higher on the three smallest tubes than on the largest diameter tube and the flat substrate (2.9 mm: $111.68 \pm$

50.94 mN, 5 mm: 129.49 ± 47.87 mN, 11.9 mm: 125.96 ± 61.62 mN; Kruskal–Wallis ANOVA on ranks, $H=40.05$, d.f.=4, $P<0.001$, $N=14$; Tukey's test, $P<0.05$). The median of the pull-off forces was highest on the 5.0 mm diameter tube, similar to *S. inexpectata*, but the difference between the forces on 5.0 mm and the other small substrate diameters was not significant (Tukey's test, $P>0.05$). The mean pull-off force on the 24.8 mm diameter tube (67.41 ± 31.30 mN) was higher than that on the flat substrate (35.27 ± 14.62 mN); however, this difference was also statistically not significant (Kruskal–Wallis ANOVA on ranks, $H=40.05$, d.f.=4, $P<0.001$, $N=14$; Tukey's test, $P>0.05$). In contrast to the traction forces, both species revealed increasing pull-off forces on decreasing tube diameter, with the maximum on the 5.0 mm tube and decreasing pull-off forces for tubes thinner than 5.0 mm.

Comparison of attachment forces between species

The adult females of *O. mouhotii* (0.91 ± 0.22 g, $N=14$) were lighter than those of *S. inexpectata* (1.18 ± 0.26 g, $N=14$; t -test, $t=3.09$, d.f.=13, $P=0.009$). Therefore, for comparing traction and pull-off forces of the two species with different tarsal lengths, safety factors (attachment force/body weight) were used (Fig. 6A,B). The safety factor in the traction direction was higher for *S. inexpectata* (9.17 ± 4.13) in comparison to *O. mouhotii* (5.89 ± 3.22) on the 2.9 mm tube (t -test, $t=2.337$, d.f.=26, $N_{1,2}=14$, $P=0.014$). On all other substrates, the differences between the specific safety factors were not

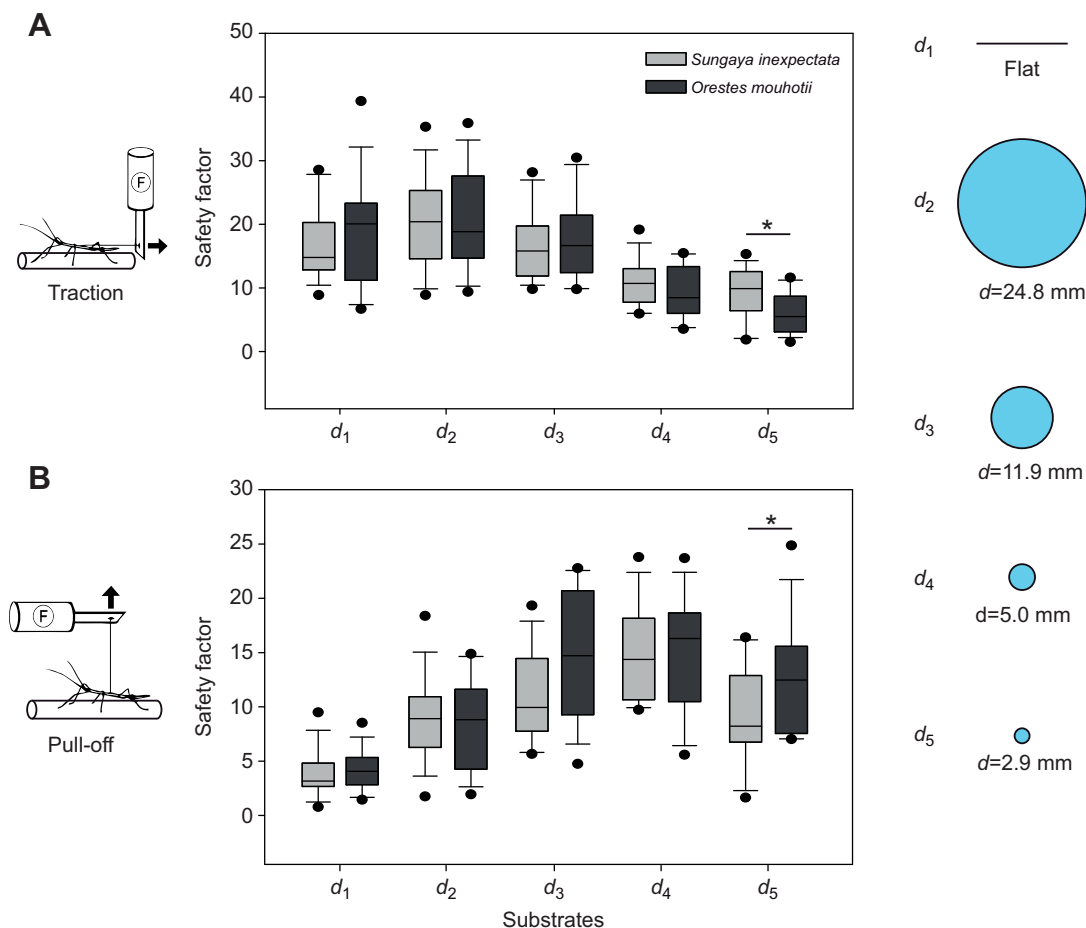


Fig. 6. Comparison of safety factors in the traction and pull-off direction between the two species on the differently curved substrates. (A) Traction ($N=14$ for both). (B) Pull-off ($N=14$ for both). Boxes indicate the 25th and 75th percentiles, whiskers are the 10th and 90th percentiles and the line within the boxes shows the median. * $P<0.05$, only significant comparisons are displayed. (C) The different substrates.

significant. In contrast, comparison of safety factors in the pull-off direction revealed a significantly higher safety factor on the 2.9 mm tube for *O. mouhotii* (t -test, $t=-2.149$, d.f.=26, $N_{1,2}=14$, $P=0.021$) (Fig. 6B). Although the safety factors in the pull-off direction on the 11.9 mm diameter tube were different for the species (*O. mouhotii*: 14.27 ± 5.89 , *S. inexpectata*: 11.05 ± 4.12), the t -test probability value was slightly higher than 0.05 (t -test, $t=-1.666$, d.f.=26, $N_{1,2}=14$, $P=0.054$).

DISCUSSION

Tarsal morphology

In some stick insect species, the length of the tarsi differs between the three leg pairs (Poinar, 2011; Vallotto et al., 2016, measured from fig. 2 therein). We did not find a significant difference in the total tarsal length between different leg pairs in the two species of Heteropterygidae examined herein, but difference occurred between the species. In the following, we discuss the functional relevance of the different tarsal lengths in regard to the attachment performance on curved substrates. Other insects use tibial spurs for locomotion on curved substrates, either for interlocking with the stem (Gladun and Gorb, 2007) or in combination with the pretarsal claws to generate traction even on smooth curved substrates (Bußhardt et al., 2014). Such structures are not present in the species examined herein.

Attachment performance on curved substrates

In the vertical direction, the generated pull-off force of both species increased with the degree of curvature, from the flat substrate to the 5.0 mm diameter tube. On the thinnest tube, the pull-off forces were again reduced (see Fig. 4B,D). Accordingly, there is an optimal range of stem diameter, where the stick insect generates the strongest attachment, and despite the different tarsal lengths, this range was surprisingly similar for the two species. Furthermore, in both species, the generated pull-off force on the three smallest tubes, even on the thinnest one (2.9 mm diameter), was significantly higher than that on the flat plate.

On curved substrates, the increasing attachment performance can be caused by generation of active adduction forces. When climbing on thin rods, compared with their own body size, animals can utilize clamping grips and generate active adduction forces to increase normal load on the surface. This has been shown for tree frogs (Endlein et al., 2017; Hill et al., 2018) and was additionally assumed for sawyer beetles (Voigt et al., 2017) and other insect species from different lineages (Gladun and Gorb, 2007). The angle between the substrate surface and the direction of pulling obviously influences the pull-off force. According to Kendall's peeling model, the pulling force is dependent on the peeling angle (Kendall, 1975). Insect attachment systems are usually more complex than Kendall's classical peeling model predicts (Gorb and Heepe, 2017; Heepe et al., 2017); still, there is a significant influence of the angle between substrate and the detaching tarsus in many animals (Gu et al., 2016). The relationship between peeling angle and attachment force has been previously shown in Hymenoptera (Federle et al., 2001), Diptera (Niederegger et al., 2002) and Blattodea (Clemente and Federle, 2008), as well as in vertebrates, such as geckos (Autumn et al., 2000; Persson and Gorb, 2003) and frogs (Hanna and Barnes, 1991).

In the species examined herein, leg and tarsus orientation on a curved tube caused a lower angle between the attachment pads and the direction of pulling with increasing curvature of the substrate (Fig. 4), resulting in a higher amount of force, which is necessary for detachment of the attachment pad. This relationship is also reflected

by the AoA: a larger AoA of the animal on the substrate results in more individual attachment pads in contact with the surface, with the pulling force acting at a correspondingly lower angle. Consequently, a higher AoA results in a higher pull-off force, except for the smallest tube. The pull-off force on the smallest tube (2.9 mm diameter) was significantly lower than on the 5.0 mm diameter tube in *S. inexpectata* (in *O. mouhotii*, the median of the pull-off force was lower as well, but not statistically significant). Additionally, the walking gait pattern of both species revealed a larger percentage of the tetrapod gait. The tetrapod gait in comparison to the tripod gait often indicates a less secure attachment to the substrate in insects (Gorb and Heepe, 2017; Büscher and Gorb, 2019). On curved substrates with a very low diameter, the flexion of the tarsal chain is not sufficient to bring all attachment pads into contact with the substrate and hence results in a lower pull-off force. However, *S. inexpectata* is able to contact the 2.9 mm diameter tube with the arolium and two euplantulae (Fig. 4C).

In contrast to the pull-off forces, the traction forces were higher for larger tube diameters and decreased with decreasing tube diameter for both species (Fig. 5A,C). The traction forces were highest on curved substrates with large diameters (24.8 mm). The curvature of the substrate potentially enables the tarsi to better adapt to the surface profile than on flat substrates. Additionally, the convex substrate curvature provides better grasping of the substrate and the generation of higher load on the tarsi in comparison to flat substrates (Frantsevich and Cruse, 1997; Gladun and Gorb, 2007; Voigt et al., 2017). On very thin stems, with similar or lower diameter than the tarsal length, the examined species provide lower traction force than on surfaces with a lower degree of curvature. Generally, on the smaller tubes, especially on the thinnest ones, fewer attachment pads were brought into contact and, hence, less actual contact area was provided, resulting in lower attachment force (Arzt et al., 2003; Persson and Gorb, 2003). Presumably, on smaller diameter tubes, less contact area is available to distribute the resulting forces, especially in the lateral dimension. This probably results in a reduced stabilization on the thinner tubes in comparison with the larger ones, leading to a faster detachment of single legs and a lower attachment force in general. Additionally, in animals that clamp their tarsi around the tubes, the traction force vector along the substrate is oriented perpendicular to the orientation of the tarsus. Accordingly, the tarsi are sliding in the lateral direction in most cases. If the tarsi were arranged differently, the animals actively positioned them along the tube and tried to counteract the pulling direction. Previous studies have reported higher friction for stick insect euplantulae while being pulled compared with being pushed (Bußhardt et al., 2012). In the lateral direction of the euplantula, to the best of our knowledge, nothing is known about the frictional properties of the attachment pad in stick insects. The generated traction force, however, is significantly lower on the smaller tubes, where the tarsi cannot be arranged along the tube length, in comparison to the flat substrate and the tubes with larger diameters (Fig. 5A,C).

Influence of tarsal length on attachment on curved substrates

In both directions (vertical and horizontal pulling), the two species showed similar trends, i.e. higher pull-off force on thinner stems and higher traction on thicker stems and flat substrates. The safety factors of both species were similar and not statistically different on all substrates except the 2.9 mm diameter tube. Hence, the length of the tarsus essentially does not matter for stems with larger diameters

than the tarsal length. Only on the thinnest tube (2.9 mm diameter) was the safety factor of *S. inexpectata* in the traction direction higher than for *O. mouhotii* and lower in the pull-off direction (Fig. 6). The shorter tarsi of *O. mouhotii* can generate a larger AoA in comparison to the longer tarsi of *S. inexpectata*. This results in a lower angle between the tarsus and tibia and, hence, could explain the higher safety factor of *O. mouhotii* in the pull-off direction (e.g. Gu et al., 2016). In spite of the longer tarsus of *S. inexpectata*, it does not allow for a proper grasping around the rod, as the tarsus is not flexible enough to follow the perimeter of the substrate. The tarsus of *O. mouhotii*, however, is able to bring all attachment pads into contact.

Opiliones (Arachnida), or harvestmen, are able to provide friction using their elongated and highly articulated prehensile feet (Wolff et al., 2019). In contrast to harvestmen, stick insects, like most other insects, are not able to hyperflex the tarsus and therefore need to provide load by the coordinated action of contralateral legs (Gladun and Gorb, 2007; Bußhardt et al., 2014; Voigt et al., 2017). The safety factor in the traction direction was higher for *S. inexpectata* on the substrate with the smallest diameter. The tarsi of this species made contact with the substrate at a lower AoA than those of *O. mouhotii* (Fig. 4), i.e. >90 deg but <180 deg. This results in potentially better clamping and higher adduction forces of the contralateral legs, and consequently, higher traction, as the traction is dependent on the load on the attachment pads (e.g. Gorb and Scherge, 2000; Gorb et al., 2000; Bußhardt et al., 2012; Gorb, 2007; Labonte and Federle, 2013; Labonte et al., 2014). In *O. mouhotii*, in contrast, the high AoA (>180 deg) on the small tube results in lower adduction forces, as the tarsus grasps around the tube. The force transmitted to the attachment pads is, in this conformation, not generating load, as the tarsus is under tension. This is in agreement with observations previously made on other insects, which clasp stems with an equal or slightly larger diameter than the tarsal length, but clutch stems with a smaller diameter with the contralateral tarsi (Gladun and Gorb, 2007), and, as shown for the two species examined herein, this clutching results in higher traction.

Usage of the attachment system for locomotion on curved substrates

According to Federle and Endlein (2004), attachment is regulated on four different hierarchical levels, ranging from control of the attachment system itself, over movements of the tarsomeres/tarsi and the legs, to the body kinematics. Some aspects of the tarsus, leg and body positioning have already been discussed above. Furthermore, there are some behavioural aspects influencing body kinematics in addition to the walking gait patterns and posture (Table 1). Generally, the clamping efficiency is dependent on morphological characteristics; for example, the ratios of body width and leg length (Voigt et al., 2017). The same ratios are reported to show a correlation of behaviour and morphology, i.e. while climbing on stairs, stick insect species with shorter legs show different behaviour from species with long legs (Theunissen et al., 2015).

With respect to their body lengths, the legs of *S. inexpectata* are longer than those of *O. mouhotii*. Both are associated with low-growing vegetation and show quite similar feeding habits and bury their eggs in the soil (Büscher et al., 2019). However, there are no studies that have investigated details of their natural behaviour in the field. Still, the tarsi of *O. mouhotii* are shorter and therefore perform better on thin branches than those of *S. inexpectata*. Presumably, the tarsi of *O. mouhotii* are adapted to locomote on low-growing vegetation with small stem diameter, rather than larger plant diameters (bushes and trees).

In lizards (Goodmann et al., 2008) and *Stenus* rove beetles (Betz, 2006) limb length and habitat correlate in some species, e.g. limb length increases with perch diameter or habitat openness (presence of less suitable refugia in the habitat). Likewise, openness in the natural habitats could be higher for *S. inexpectata* than for *O. mouhotii* and therefore longer legs (and tarsi) could be a result of the presence of larger substrate diameters and less-suitable twigs for imitation in the natural habitats of *S. inexpectata*.

Ground-dwelling spiders with longer legs walk faster on curved substrates with large diameter compared with flat substrates and thin stems (Prenter et al., 2010). Similarly, *S. inexpectata* has longer limbs and does not show any cataleptic defensive reaction and instead tries to escape. *Orestes mouhotii* in contrast relies on its camouflage in combination with thanatosis (Bedford, 1978). For the employment of visual camouflage, next to the animal's size, structure and colour of the habitat play a major role, as shown for chameleons (Cuadrado et al., 2001) and moths (Kang et al., 2015).

Orestes mouhotii combines smaller size and stronger crypsis compared with *S. inexpectata*, which might be a part of the predator avoidance strategy of this species. Traction forces, however, were larger for longer tarsi on some substrates. Higher speed during locomotion and active escape reactions might be assumed as potential behavioural traits associated with the longer tarsal length.

Conclusions

This study sheds light on the attachment performance of stick insects on curved substrates and provides, to the best of our knowledge, the first quantitative data on traction and pull-off forces for this group of insects on smooth rods of different diameter. Stick and leaf insects face several different surface topographies in their natural habitats, and dominant among these are twigs and branches of different diameter. The degree of substrate curvature has a significant influence on the attachment ability of both examined species, namely higher traction on curved substrates with larger diameters and higher pull-off force on substrates with lower diameter. On flat substrates and curved substrates with large diameters, the two species showed similar traction performance and much lower pull-off forces than on curved substrates. The traction force decreases with decreasing stem diameter and the pull-off force increases with decreasing stem diameter, unless the substrate is thinner than the tarsal length. On flat substrates and curved substrates with large diameters, the tarsus length does not significantly influence the attachment ability. On stems with diameters lower than the length of the tarsus, the pull-off forces are reduced, as the contact formation between tarsal attachment pads and the substrate is reduced. Traction forces, however, are larger for longer tarsi on stems with a diameter falling below the length of the tarsus, as the longer tarsi can better clamp onto the substrate between the contralateral tarsi and produce higher adduction forces, while shorter tarsi clasp around the stem. The attachment performance is also dependent on the number of tarsi and tarsomeres in contact, tarsus position on the tube (e.g. AoA), tarsus and leg orientation, as well as leg and body configuration on the surface.

Corroborating earlier studies on other insects (e.g. Federle et al., 2001; Niederegger et al., 2002; Clemente and Federle, 2008), the pull-off force is dependent on the tibiotarsal angle. On rods, the pull-off force is higher for higher AoA (or lower tibiotarsal angle). Furthermore, the AoA probably influences adduction forces, leading to proper load transmission on the euplantulae, which in turn influences the traction force. Additionally, the contribution of claws (Song et al., 2016; Büscher and Gorb, 2019) as well as differences in the euplantular attachment microstructures present in

other stick insect species (Büscher et al., 2018a,b, 2019) might also influence the attachment performance on curved rough substrates.

Surfaces with different degrees of curvature play an important role for stick insects. Referring to the results of this study, this induces a much more complex interaction of various phenomena. The results presented herein further stress the importance of evaluation of attachment performance on different surface geometries (Gladun and Gorb 2007; Bußhardt et al., 2014; Voigt et al., 2017, 2019), besides commonly investigated flat substrates. Furthermore, insights generated from the present experiments on curved substrates can be potentially useful for the design of bio-inspired robotic grippers (e.g. Gorb et al., 2007; Voigt et al., 2012).

Acknowledgements

We thank Chuchu Li and Dennis Petersen (Department of Functional Morphology and Biomechanics, Kiel University, Germany) for fruitful discussions and Femke Vogel (same affiliation) for assistance with force measurements. Furthermore, we thank Holger Dräger (Schwerin, Germany) and Daniel Dittmar (Berlin, Germany) for providing the breeding stocks used for the laboratory cultures.

Competing interests

The authors declare no competing or financial interests.

Author contributions

Conceptualization: T.H.B., S.N.G.; Methodology: T.H.B., S.N.G.; Validation: T.H.B., S.N.G.; Formal analysis: T.H.B., M.B.; Investigation: T.H.B., M.B.; Resources: T.H.B., S.N.G.; Writing - original draft: T.H.B.; Writing - review & editing: T.H.B., M.B., S.N.G.; Visualization: T.H.B., M.B.; Supervision: T.H.B., S.N.G.; Project administration: T.H.B., S.N.G.; Funding acquisition: S.N.G.

Funding

Funding was provided by the Deutsche Forschungsgemeinschaft (grant GO 995/34-1).

Supplementary information

Supplementary information available online at <https://jeb.biologists.org/lookup/doi/10.1242/jeb.226514.supplemental>

References

- Autumn, K., Liang, Y., Hsieh, S., Zesch, W., Chan, W. P., Kenny, T. W., Fearing, R. and Full, R. J.** (2000). Adhesive force of a single gecko foot-hair. *Nature* **405**, 681-685. doi:10.1038/35015073
- Arzt, E., Gorb, S. N. and Spolenak, R.** (2003). From micro to nano contacts in biological attachment devices. *Proc. Nat. Acad. Sci. USA* **100**, 10603-10606. doi:10.1073/pnas.1534701100
- Bedford, G. O.** (1978). Biology and ecology of the Phasmatodea. *Ann. Rev. Entomol.* **23**, 125-149. doi:10.1146/annurev.en.23.010178.001013
- Bennemann, M., Scholz, I. and Baumgartner, W.** (2011). Functional morphology of the adhesive organs of stick insects (*Carausius morosus*). *Proc. SPIE* **7975**, 79751A-1.
- Beutel, R. G. and Gorb, S. N.** (2001). Ultrastructure of attachment specializations of hexapods (Arthropoda). Evolutionary patterns inferred from a revised ordinal phylogeny. *J. Zool. Syst. Evol. Res.* **39**, 177-207.
- Beutel, R. G. and Gorb, S. N.** (2006). A revised interpretation of the evolution of attachment structures in Hexapoda with special emphasis on Mantophasmatodea. *Arthropod Syst. Phylogeny* **64**, 3-25.
- Beutel, R. G. and Gorb, S. N.** (2008). Evolutionary scenarios for unusual attachment devices of Phasmatodea and Mantophasmatodea (Insecta). *Sys. Ent.* **33**, 501-510. doi:10.1111/j.1365-3113.2008.00428.x
- Betz, O.** (2002). Performance and adaptive value of tarsal morphology in rove beetles of the genus *Stenus* (Coleoptera, Staphylinidae). *J. Exp. Biol.* **205**, 1097-1113.
- Betz, O.** (2006). Der Anpassungswert morphologischer Strukturen: Integration von Form, Funktion und Ökologie am Beispiel der Kurzflügelkäfer-Gattung *Stenus* (Coleoptera, Staphylinidae). *Entomologie Heute* **18**, 3-26.
- Bijma, N. N., Gorb, S. N. and Kleinteich, T.** (2016). Landing on branches in the frog *Trachycephalus resinifictrix* (Anura: Hylidae). *J. Comp. Physiol. A* **202**, 267-276.
- Büscher, T. H. and Gorb, S. N.** (2017). Subdivision of the neotropical Prisopodinae Brunner von Wattenwyl 1893 based on features of tarsal attachment pads (Insecta: Phasmatodea). *Zookeys* **645**, 1-11. doi:10.1007/s00359-016-1069-0
- Büscher, T. H. and Gorb, S. N.** (2019). Complementary effect of attachment devices in stick insects (Phasmatodea). *J. Exp. Biol.* **222**, jeb209833. doi:10.1242/jeb.209833
- Büscher, T. H., Buckley, T. R., Grohmann, C., Gorb, S. N. and Bradler, S.** (2018a). The evolution of tarsal adhesive microstructures in stick and leaf insects (Phasmatodea). *Front. Ecol. Evol.* **6**, 69. doi:10.3389/fevo.2018.00069
- Büscher, T. H., Kryuchkov, M., Katanaev, V. L. and Gorb, S. N.** (2018b). Versatility of Turing patterns potentiates rapid evolution in tarsal attachment microstructures of stick and leaf insects (Phasmatodea). *J. R. Soc. Interface* **15**, 20180281. doi:10.1098/rsif.2018.0281
- Büscher, T. H., Grohmann, C., Bradler, S. and Gorb, S. N.** (2019). Tarsal attachment pads in Phasmatodea (Hexapoda: Insecta). *Zoologica* **164**, 1-94.
- Bußhardt, P., Wolf, H. and Gorb, S. N.** (2012). Adhesive and frictional properties of tarsal attachment pads in two species of stick insects (Phasmatodea) with smooth and nubby euplantulæ. *Zoology* **115**, 135-141. doi:10.1016/j.zool.2011.11.002
- Bußhardt, P., Kunze, D. and Gorb, S. N.** (2014). Interlocking-based attachment during locomotion in the beetle *Pachnoda marginata* (Coleoptera, Scarabaeidae). *Sci. Rep.* **4**, 6998. doi:10.1038/srep06998
- Bradler, S. and Buckley, T. R.** (2018). Biodiversity of phasmatodea. In *Insect Biodiversity: Science and Society*, Vol. 2, (ed. R. G. Foottit and P. H. Adler), pp. 281-313. Hoboken, NJ: Wiley-Blackwell.
- Brock, P. D., Büscher, T. H. and Baker, E.** (2019). Phasmida Species File (version 5.0). In *Species 2000 & ITIS Catalogue of Life, 2019 Annual Checklist* (ed. Y. Roskov, G. Ower, T. Orrell, D. Nicolson, N. Bailly, P.M. Kirk, T. Bourgoin, R.E. DeWalt, W. Decock, E. van Nieukerken et al.). Leiden: Species 2000: Naturalis ISSN 2405-8858.
- Clemente, C. J. and Federle, W.** (2008). Pushing versus pulling: division of labour between tarsal attachment pads in cockroaches. *Proc. R. Soc. Lond. B* **275**, 1329-1336. doi:10.1098/rspb.2007.1660
- Cuadrado, M., Martin, J. and López, P.** (2001). Camouflage and escape decisions in the common chameleon *Chamaeleo chamaeleo*. *Biol. J. Linn. Soc. Lond.* **72**, 547-554. doi:10.1111/j.1095-8312.2001.tb01337.x
- Endlein, T., Ji, A., Yuan, S., Hill, I., Wang, H., Barnes, W. J. P., Dai, Z. and Sitti, M.** (2017). The use of clamping grips and friction pads by tree frogs for climbing curved surfaces. *Proc. R. Soc. B* **284**, 20162867. doi:10.1098/rspb.2016.2867
- Federle, W. and Endlein, T.** (2004). Locomotion and adhesion: dynamic control of adhesive surface contact in ants. *Arthropod Struct. Dev.* **33**, 67-75. doi:10.1016/j.asd.2003.11.001
- Federle, W., Brainerd, E. L., McMahon, T. A. and Hölldobler, B.** (2001). Biomechanics of the movable pretarsal adhesive organ in ants and bees. *Proc. Natl. Acad. Sci. USA* **98**, 6215-6220. doi:10.1073/pnas.111139298
- Frantsevich, L. and Cruse, H.** (1997). The stick insect, *Oribimus asperimus* (Phasmida, Bacillidae) walking on different surfaces. *J. Ins. Physiol.* **43**, 447-455. doi:10.1016/S0022-1910(96)00119-9
- Gladun, D. and Gorb, S. N.** (2007). Insect walking techniques on thin stems. *Arthropod Plant Interact.* **1**, 77-91. doi:10.1007/s11829-007-9007-2
- Goodmann, B. A., Miles, D. B. and Schwarzkopf, L.** (2008). Life on the rocks: habitat use drives morphological and performance evolution in lizards. *Ecology* **89**, 3462-3471. doi:10.1890/07-2093.1
- Gorb, S. N.** (2001). *Attachment Devices of Insect Cuticle*. Dordrecht, the Netherlands: Springer.
- Gorb, S. N.** (2007). Smooth attachment devices in insects: functional morphology and biomechanics. *Adv. In Insect Phys.* **34**, 81-115. doi:10.1016/S0065-2806(07)34002-2
- Gorb, S. N. and Gorb, E. V.** (2004). Ontogenesis of the attachment ability in the bug *Coreus marginatus* (Heteroptera, Insecta). *J. Exp. Biol.* **207**, 2917-2924. doi:10.1242/jeb.01127
- Gorb, S. N. and Heepe, L.** (2017). Biological fibrillar adhesives: Functional principles and biomimetic applications. In *Handbook of Adhesion Technology* (ed. L. da Silva, A. Öchsner and R. Adams), pp. 1-37. Cham: Springer.
- Gorb, S. N. and Scherge, M.** (2000). Biological microtribology: anisotropy in frictional forces of orthopteran attachment pads reflects the ultrastructure of a highly deformable material. *Proc. R. Soc. Lond. B* **267**, 1239-1244. doi:10.1098/rspb.2000.1133
- Gorb, S. N., Jiao, Y. and Scherge, M.** (2000). Ultrastructural architecture and mechanical properties of attachment pads in *Tettigonia viridissima* (Orthoptera Tettigoniidae). *J. Comp. Physiol. A* **186**, 821-831. doi:10.1007/s003590000135
- Gorb, S. N., Varenberg, M., Peressadko, A. and Tuma, A.** (2007). Biomimetic mushroom-shaped fibrillar adhesive microstructure. *J. R. Soc. Interface* **4**, 271-275. doi:10.1098/rsif.2006.0164
- Gottardo, M., Vallotto, D. and Beutel, R. G.** (2015). Giant stick insects reveal unique ontogenetic changes in biological attachment devices. *Arthropod Str. Dev.* **44**, 195-199. doi:10.1016/j.asd.2015.01.001
- Grabowska, M., Godlewska, E., Schmidt, J. and Daun-Gruhn, S.** (2012). Quadrupedal gaits in hexapod animals - inter-leg coordination in free-walking adult stick insects. *J. Exp. Biol.* **215**, 4255-4266. doi:10.1242/jeb.073643
- Gu, Z., Li, S., Zhang, F. and Wang, S.** (2016). Understanding surface adhesion in nature: a peeling model. *Adv. Sci.* **3**, 1500327. doi:10.1002/adv.201500327
- Hanna, G. J. W. and Barnes, W. J.** (1991). Adhesion and detachment of the toe pads of tree frogs. *J. Exp. Biol.* **155**, 103-125.
- Heepe, L., Raguseo, S. and Gorb, S. N.** (2017). An experimental study of double-peeling mechanism inspired by biological adhesive systems. *Appl. Phys. A* **123**, 124. doi:10.1007/s00339-016-0753-9

- Hill, I. D. C., Dong, B., Barnes, W. J. P., Ji, A. and Endlein, T. (2018). The biomechanics of tree frogs climbing curved surfaces: a gripping problem. *J. Exp. Biol.* **221**, jeb168179. doi:10.1242/jeb.168179
- Kang, C., Stevens, M., Moon, J., Lee, S.-I. and Jablonski, P. G. (2015). Camouflage through behavior in moths: the role of background matching and disruptive coloration. *Behav. Ecol.* **221**, 45-54. doi:10.1093/behecol/aru150
- Kendall, K. (1975). Thin film peeling—the elastic term. *J. Phys. D: Appl. Phys.* **8**, 1449. doi:10.1088/0022-3727/8/13/005
- Labonte, D. and Federle, W. (2013). Functionally different pads on the same foot allow control of attachment: stick insects have load-sensitive “heel” pads for friction and shear-sensitive “toe” pads for adhesion. *PLoS ONE* **8**, e81943. doi:10.1371/journal.pone.0081943
- Labonte, D., Williams, J. A. and Federle, W. (2014). Surface contact and design of fibrillar ‘friction pads’ in stick insects (*Carausius morosus*): mechanisms for large friction coefficients and negligible adhesion. *J. R. Soc. Interface* **11**, 20140034. doi:10.1098/rsif.2014.0034
- Labonte, D., Struecker, M.-Y., Birn-Jeffery, A. V. and Federle, W. (2019). Shear-sensitive adhesion enables size-independent adhesive performance in stick insects. *Proc. R. Soc. B* **286**, 20191327. doi:10.1098/rspb.2019.1327
- Niederegger, S., Gorb, S. N. and Jiao, Y. (2002). Contact behaviour of tenent setae in attachment pads of the blowfly *Calliphora vicina* (Diptera, Calliphoridae). *J. Comp. Physiol. A* **187**, 961-970. doi:10.1007/s00359-001-0265-7
- Persson, B. N. J. and Gorb, S. N. (2003). The effect of surface roughness on the adhesion of elastic plates with application to biological systems. *J. Chem. Phys.* **119**, 11437-11444. doi:10.1063/1.1621854
- Pohl, H. (2010). A scanning electron microscopy specimen holder for viewing different angles of a single specimen. *Microsc. Res. Tech.* **73**, 1073-1076. doi:10.1002/jemt.20835
- Poinar, G., Jr (2011). A walking stick, *Clonistria dominicana* n. sp. (Phasmatodea: Diapheromeridae) in Dominican amber. *Hist. Biol.* **23**, 223-226. doi:10.1080/08912963.2010.522405
- Prenter, J., Pérez-Staples, D. and Taylor, P. W. (2010). The effects of morphology and substrate diameter on climbing and locomotor performance in male spider. *Funct. Ecol.* **24**, 400-408. doi:10.1111/j.1365-2435.2009.01633.x
- Robertson, J. A., Bradler, S. and Whiting, M. F. (2018). Evolution of oviposition techniques in stick and leaf insects (Phasmatodea). *Front. Ecol. Evol.* **6**, 216. doi:10.3389/fevo.2018.00216
- Song, Y., Dai, Z., Ji, A. and Gorb, S. N. (2016). The synergy between the insect-inspired claws and adhesive pads increases the attachment ability on various rough surfaces. *Sci. Rep.* **6**, 26219. doi:10.1038/srep26219
- Theunissen, L. M., Bekemeier, H. H. and Dürr, V. (2015). Comparative whole-body kinematics of closely related insect species with different body morphology. *J. Exp. Biol.* **218**, 340-352. doi:10.1242/jeb.114173
- Vallotto, D., Bresseel, J., Heitzmann, T. and Gottardo, M. (2016). A black-and-red stick insect from the Philippines - observations on the external anatomy and natural history of a new species of *Orthomeria*. *Zookeys* **559**, 35-57. doi:10.3897/zookeys.559.6281
- Voigt, D., Karguth, A. and Gorb, S. N. (2012). Shoe soles for the grip-ping robot: searching for polymer-based materials maxi-mising friction. *Robot. Auton. Syst.* **60**, 1046-1055. doi:10.1016/j.robot.2012.05.012
- Voigt, D., Takanashi, T., Tsuchihara, K., Yazaki, K., Kuroda, K., Tsubaki, R. and Hosoda, N. (2017). Strongest grip on the rod: tarsal morphology and attachment of Japanese pine sawyer beetles. *Zool. Lett.* **3**, 16. doi:10.1186/s40851-017-0076-5
- Voigt, D., Goodwyn, P., Sudo, M., Fujisaki, K. and Varenberg, M. (2019). Gripping ease in southern green stink bugs *Nezara viridula* L. (Heteroptera: Pentatomidae): Coping with geometry, orientation and surface wettability of substrate. *Entomol. Sci.* **22**, 105-118.
- Wang, M., Béthoux, O., Bradler, S., Jacques, F. M. B., Cui, Y. and Ren, D. (2014). Under cover at pre-angiosperm times: a cloaked phasmatodean insect from the Early Cretaceous Jehol biota. *PLoS ONE* **9**, e91290. doi:10.1371/journal.pone.0091290
- Wohlfart, E., Wolff, J. O., Arzt, E. and Gorb, S. N. (2014). The whole is more than the sum of all its parts: collective effect of spider attachment organs. *J. Exp. Biol.* **217**, 222-224. doi:10.1242/jeb.093468
- Wolff, J. O. and Gorb, S. N. (2012). The influence of humidity on the attachment ability of the spider *Philodromus dispar* (Araneae, Philodromidae). *Proc. R. Soc. B* **279**, 139-143. doi:10.1098/rspb.2011.0505
- Wolff, J. O., Wiegmann, C., Wirkner, C. S., Koehnsen, A. and Gorb, S. N. (2019). Traction reinforcement in prehensile feet of harvestmen (Arachnida, Opiliones). *J. Exp. Biol.* **222**, jeb192187. doi:10.1242/jeb.192187

Table S1. Measurements of all tarsomeres and the total length of the hind tarsus for *Orestes mouhotii* and *Sungaya inexpectata* ($N_{1,2} = 11$).

species	ID	T1 [mm]	T2 [mm]	T3 [mm]	T4 [mm]	T5 [mm]	Lenght [mm]
<i>Orestes mouhotii</i>	#OM1	1.00	0.47	0.45	0.50	1.06	3.48
<i>Orestes mouhotii</i>	#OM2	0.90	0.42	0.41	0.45	0.95	3.13
<i>Orestes mouhotii</i>	#OM3	1.09	0.51	0.50	0.55	1.16	3.81
<i>Orestes mouhotii</i>	#OM4	0.88	0.41	0.40	0.44	0.93	3.06
<i>Orestes mouhotii</i>	#OM5	1.02	0.48	0.46	0.51	1.08	3.54
<i>Orestes mouhotii</i>	#OM6	0.80	0.37	0.36	0.40	0.85	2.79
<i>Orestes mouhotii</i>	#OM7	1.05	0.49	0.48	0.52	1.11	3.65
<i>Orestes mouhotii</i>	#OM8	1.09	0.51	0.50	0.55	1.16	3.80
<i>Orestes mouhotii</i>	#OM9	1.00	0.47	0.45	0.50	1.06	3.47
<i>Orestes mouhotii</i>	#OM10	0.82	0.38	0.37	0.41	0.87	2.85
<i>Orestes mouhotii</i>	#OM11	0.92	0.43	0.42	0.46	0.98	3.21
<i>Sungaya inexpectata</i>	#SI1	2.91	0.96	0.88	0.92	2.20	7.87
<i>Sungaya inexpectata</i>	#SI2	2.88	0.95	0.88	0.91	2.18	7.80
<i>Sungaya inexpectata</i>	#SI3	2.72	0.90	0.83	0.85	2.05	7.35
<i>Sungaya inexpectata</i>	#SI4	2.98	0.99	0.91	0.94	2.26	8.07
<i>Sungaya inexpectata</i>	#SI5	2.76	0.91	0.84	0.87	2.09	7.46
<i>Sungaya inexpectata</i>	#SI6	2.93	0.97	0.89	0.92	2.22	7.94
<i>Sungaya inexpectata</i>	#SI7	2.90	0.96	0.88	0.91	2.20	7.85
<i>Sungaya inexpectata</i>	#SI8	3.09	1.02	0.94	0.97	2.34	8.35
<i>Sungaya inexpectata</i>	#SI9	2.80	0.93	0.85	0.88	2.12	7.58
<i>Sungaya inexpectata</i>	#SI10	3.16	1.04	0.96	0.99	2.39	8.54
<i>Sungaya inexpectata</i>	#SI11	3.05	1.01	0.93	0.96	2.31	8.26

Table S2. Measurements of the total length of the tarsi of all three leg pairs for *Orestes mouhotii* and *Sungaya inexpectata* ($N_{1,2} = 15$).

species	ID	Total length [mm]		
		foreleg	midleg	hindleg
<i>Sungaya inexpectata</i>	#SI12	6.6	6.3	7.2
<i>Sungaya inexpectata</i>	#SI13	6.8	6.6	6.7
<i>Sungaya inexpectata</i>	#SI14	6.6	6.8	6.9
<i>Sungaya inexpectata</i>	#SI15	7.0	6.8	7.0
<i>Sungaya inexpectata</i>	#SI16	6.2	6.2	6.2
<i>Sungaya inexpectata</i>	#SI17	6.8	6.7	7.0
<i>Sungaya inexpectata</i>	#SI18	6.8	6.3	6.5
<i>Sungaya inexpectata</i>	#SI19	6.9	6.5	6.8
<i>Sungaya inexpectata</i>	#SI20	6.2	6.7	6.8
<i>Sungaya inexpectata</i>	#SI21	6.3	6.7	6.7
<i>Sungaya inexpectata</i>	#SI22	7.0	6.5	6.9
<i>Sungaya inexpectata</i>	#SI23	7.1	6.8	7.1
<i>Sungaya inexpectata</i>	#SI24	6.8	6.9	6.3
<i>Sungaya inexpectata</i>	#SI25	6.6	6.8	6.4
<i>Sungaya inexpectata</i>	#SI26	6.5	6.7	6.8
<i>Orestes mouhotii</i>	#OM12	3.1	2.8	2.9
<i>Orestes mouhotii</i>	#OM13	3.3	3.7	3.1
<i>Orestes mouhotii</i>	#OM14	3.2	3.8	3.8
<i>Orestes mouhotii</i>	#OM15	3.5	3.5	3.5
<i>Orestes mouhotii</i>	#OM16	2.9	2.9	3.5
<i>Orestes mouhotii</i>	#OM17	3.0	3.2	3.2
<i>Orestes mouhotii</i>	#OM18	3.1	3.5	2.8
<i>Orestes mouhotii</i>	#OM19	3.5	3.7	3.6
<i>Orestes mouhotii</i>	#OM20	2.9	2.9	3.5
<i>Orestes mouhotii</i>	#OM21	3.8	3.0	3.4
<i>Orestes mouhotii</i>	#OM22	3.3	3.0	3.1
<i>Orestes mouhotii</i>	#OM23	3.4	3.4	2.9
<i>Orestes mouhotii</i>	#OM24	3.7	3.2	3.2
<i>Orestes mouhotii</i>	#OM25	3.5	3.3	3.6
<i>Orestes mouhotii</i>	#OM26	3.3	3.4	3.5